Impact of the Paleocene-Eocene thermal maximum on deep-ocean microbenthic community structure: Using rank-abundance curves to quantify paleoecological response

Amelinda E. Webb[1,2], Lindsey R. Leighton[1,3], Stephen A. Schellenberg[1], Elizabeth A. Landau[1,4], and Ellen Thomas[2,5]
[1]Department of Geological Sciences, San Diego State University, San Diego, California 92182, USA
[2]Department of Geology and Geophysics, Yale University, New Haven, Connecticut 06511, USA
[3]Department of Earth and Atmospheric Sciences, University of Alberta, Edmonton, Alberta T6G 2R3, Canada
[4]American Geophysical Union, Education and Public Affairs, Outreach, Washington, DC 20009, USA
[5]Department of Earth and Environmental Sciences, Wesleyan University, Middletown, Connecticut 06459, USA

ABSTRACT

Global climate change has often resulted in extinction events that can be quantitatively measured by taxonomic loss but are more difficult to assess in terms of ecological restructuring. We use a commonly applied ecological tool, rank-abundance curves (RACs), to evaluate the ecological response of benthic foraminiferal and ostracode communities to the Paleocene-Eocene thermal maximum, which may be seen as an analog for current and future global warming. RACs are proxies for community structure, and therefore changes in the shape of RACs allow inferences to be drawn about and quantification of ecological responses. Benthic foraminiferal communities became increasingly stressed during the Paleocene-Eocene thermal maximum, and community reorganization occurred before the taxonomically defined extinction horizon. In contrast, ostracode communities became less stressed during the same interval, reinforcing the idea that different groups of organisms respond differently to extinction events and global warming. The decoupling of ecologic impact from taxonomic impact during the Paleocene-Eocene thermal maximum reaffirms the fact that future climate change could have far-reaching effects on taxa and ecosystems and proves the importance of examining both the taxonomic and ecologic responses of communities during extinction events.

INTRODUCTION

During the next century, global warming is projected to cause the extinction of many species (Thomas et al., 2004; Trenberth et al., 2007). Past episodes of global climate change have often resulted in extinctions or the reorganization of biological communities (Bowen et al., 2006; Twitchett, 2006). The fossil record provides an ideal opportunity to examine ecosystem response to climate change, to compare this response with modern events, and to predict possible future response. We apply rank-abundance curves (RACs) to assess the ecological response of two different groups of benthic organisms, unicellular foraminifera and multicellular ostracodes, to a rapid global warming event that occurred ca. 55 Ma, the Paleocene-Eocene thermal maximum.

Extinction studies usually focus on taxonomic changes (Sepkoski et al., 1981; Thomas, 1990, 2003, 2007; Bambach et al., 2004; Bowen et al., 2006). However, the ecological impact of extinction events, as reflected by community reorganization, may be disassociated from the taxonomic impact (McGhee et al., 2004). Thus, the combination of both ecological and taxonomic data leads to a more complete understanding of the biotic response to extinction events. Descriptions of ecological effects are usually qualitative observations, since it

is difficult to quantitatively compare pre- and postextinction communities, which are, almost by definition, taxonomically different. Rank-abundance curves (RACs) are less constrained by taxonomic changes than other quantitative methods because ranks exist regardless of taxonomic identity (Fig. 1).

Stress (e.g., rapid climate change) often induces a restructuring of resource-partitioning, and thereby abundance distributions (Whittaker, 1965), but it may not result in extinctions (Gray, 1981; Belaoussoff and Kevan, 1998). A less stressed community usually has a relatively even distribution of abundances among taxa, while a more stressed community is characterized by a more uneven distribution, where a few taxa are much more abundant than all others (Fig. 1) (Bazzaz, 1975; Gray, 1981; Belaoussoff and Kevan, 1998; McGill et al., 2007). As the community recovers from the disturbance or stress, it will likely return to a more even distribution, similar to that of prestress conditions, even if the constituent taxa have changed. These patterns have been observed across communities within terrestrial (Bazzaz, 1975; Belaoussoff and Kevan, 1998; Halloy and Barratt, 2007; McGill et al., 2007) and marine systems (Gray, 1981; Belaoussoff and Kevan, 1998; Halloy and Barrat, 2007; McGill et al., 2007), and they are considered sufficiently diagnostic
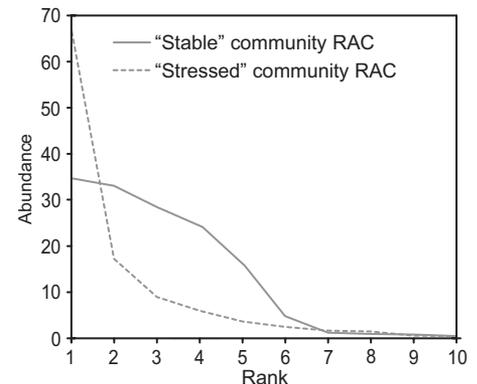
Figure 1. Hypothetical rank-abundance curves (RAC). Abundance of taxa is plotted on the *y*-axis and ranks of taxa (assigned by decreasing abundance) are plotted on the *x*-axis. Both hypothetical communities have equal abundance and richness (richness refers to the number of species [diversity] of a community). Solid line shows a relatively convex-up RAC representing a less stressed community; dashed line shows a convex-down RAC representing a more stressed community. A log scale (a commonly used method) shows a more noticeably convex-up or convex-down curve and overemphasizes the tail of the curve. We prefer this simpler, linear graphical presentation.

for RACs to have been used to assess modern ecosystem health (Gray, 1981; Belaoussoff and Kevan, 1998; Halloy and Barratt, 2007; McGill et al., 2007). The level of stress is a function of the magnitude, frequency, and unpredictability of the associated disturbances. Thus, rapid climate change on a global scale constitutes a major disturbance affecting the abundance and diversity of organisms (Gray, 1981; Belaoussoff and Kevan, 1998). Continual stress inhibits community recovery, and thus RACs generated from continuously stressed fossil communities should record the relative amount of stress to a community, even if an assemblage includes multiple generations. In contrast, if any generation begins to recover, a time-averaged fossil assemblage will have an RAC that indicates slightly lower levels of stress. When the sensitivity of

this measure is considered in the context of an extinction, which presumably reflects extreme stresses causing taxonomic loss, RACs should quantify the increasing stress leading up to, and continuing through, an extinction event.

The Paleocene-Eocene thermal maximum was an interval of extinction and faunal turnover (e.g., Bowen et al., 2006), and it may be an appropriate analog for modern and future rapid global warming (for modern details, see Trenberth et al., 2007) and thus can be used to examine biotic response to extreme climate change. During the Paleocene-Eocene thermal maximum, significant global warming was triggered by a rapid influx of isotopically light carbon into the ocean atmosphere system (for mechanisms, see Dickens, 2003; Svensen et al., 2004; Sluijs et al., 2007). Sea-surface temperatures increased by ~4–8 °C, and intermediate waters warmed by ~5 °C during the Paleocene-Eocene thermal maximum (Kennett and Stott, 1991; Zachos et al., 2003, 2006; Sluijs et al., 2007). The input of CO_2 decreased the carbonate saturation state of the ocean, producing a temporary shoaling of the lysocline and carbonate compensation depth (Zachos et al., 2005). The Paleocene-Eocene thermal maximum is readily identified by the extreme negative shift in $\delta^{13}C$ (Bains et al., 1999), referred to hereafter as the carbon isotope excursion (CIE). Many groups across marine and terrestrial realms were affected by the Paleocene-Eocene thermal maximum (see review in Bowen et al., 2006).

MATERIALS AND METHODS

We used faunal data from the most intensely studied record of the Paleocene-Eocene thermal maximum, a lower-bathyal carbonate ooze sequence drilled at Ocean Drilling Program (ODP) Site 690 on Maud Rise in the South Atlantic (Thomas, 1990; Thomas et al., 2002; Farley and Eltgroth, 2003; Bowen et al., 2006; Roehl et al., 2007). Faunal data for benthic foraminifera (Thomas, 1990, 2003) and ostracodes at the species level allowed examination of the ecological impact of the Paleocene-Eocene thermal maximum on two different groups (see Tables DR1 and DR2, and the Appendix, in the GSA Data Repository[1]). Site 690 is arguably the most complete pelagic Paleocene-Eocene thermal maximum section available and is unique because it contains sufficient abundances of both foraminifera and ostracodes for rank-abundance analyses, although ostracodes

are several orders of magnitude less abundant than foraminifera. Given differences in abundance and logistical constraints, samples have different time resolution and coverage for the two groups (see the Appendix for more details). Sample ages were calculated using the age-model of Farley and Eltgroth (2003); bulk carbonate carbon-isotope values ($\delta^{13}C$ in ‰ relative to Vienna Peedee belemnite [VPDB]) were compiled from Bains et al. (1999), Thomas et al. (2002), and Kelly et al. (2005).

RACs were generated from taxa by sample matrices and analyzed in Microsoft Excel and SYSTAT. The shape of each RAC was quantified using kurtosis, a sample-size–independent statistical measure of the peakedness or flatness of the curve. A less stressed community has a relatively flat, convex-up RAC, and therefore a lower kurtosis value, whereas a stressed community has a relatively peaked, convex-down RAC, and therefore a higher kurtosis value (Fig. 1). The fossil assemblage in each sample is hereafter referred to as a community. Evenness was calculated as Buzas and Gibson evenness (Hayek and Buzas, 1997) (see the Appendix for more details).

RESULTS

The two groups showed markedly different community-level responses through the Paleocene-Eocene thermal maximum. We divided the study interval into pre-CIE, CIE, and post-CIE intervals based on Thomas (2003) and Farley and Eltgroth (2003) (Figs. 2 and 3). Foraminifera experienced an extinction (35%–50% species loss) at the onset of the CIE (Thomas, 2003), and gradual recovery of richness through the post-CIE interval (Figs. 2A and 3A). RAC kurtosis values were low and relatively stable before markedly increasing early in the CIE, reaching a maximum ca. 54.972 Ma (Fig. 2B). As bulk carbonate $\delta^{13}C$ values recovered toward pre-CIE values, a general decrease in kurtosis preceded a slower recovery in species richness. Bulk carbonate $\delta^{13}C$ and kurtosis are significantly negatively correlated (Pearson's correlation, $R = -0.52$, $p < 0.01$), and there is an apparent ecological threshold that divides kurtosis values above and below 3 at bulk carbonate $\delta^{13}C$ values of ~1‰ (Student's one-tailed t-test, $p < 0.01$). Evenness is significantly negatively correlated with kurtosis ($R = -0.82$, $p < 0.01$), but it notably increased prior to the onset of the CIE, dropped rapidly at the onset of the CIE, and then remained variable but elevated through the remainder of the CIE and post-CIE (Fig. 2C).

Focusing on the onset of the CIE (55.01–54.96 Ma; Fig. 3, see caption for statistical significance), kurtosis rapidly increased early within the CIE, and more strongly convex-down RAC curves occur immediately after the
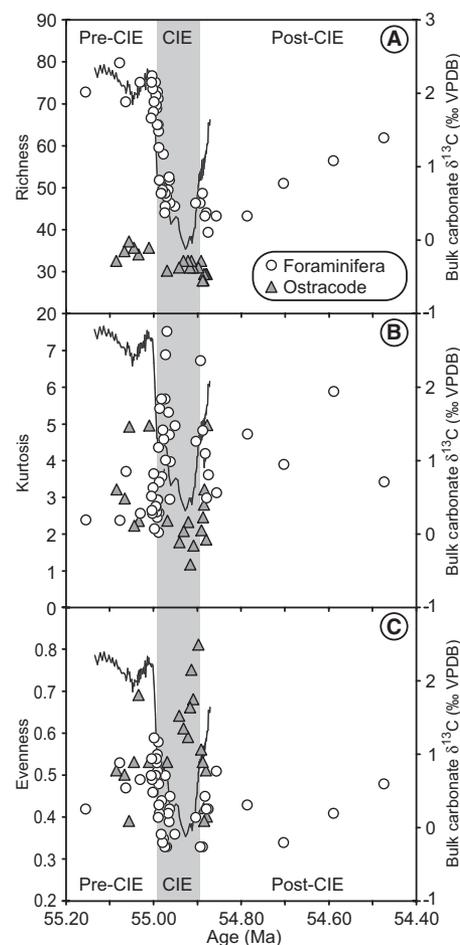
Figure 2. Benthic foraminiferal and ostracode communities across the Paleocene-Eocene thermal maximum at Ocean Drilling Program Site 690. Shading is used to differentiate the different stages of the Paleocene-Eocene thermal maximum relative to the carbon isotope excursion (CIE) (from Thomas, 1990). When ostracodes are split into two groups of communities, within and outside the CIE (either before onset or after the recovery), kurtosis is significantly different (Student's one-tailed t-test, $p < 0.05$)—communities within the CIE have a more convex-down curve shape than communities below or above the CIE.

largest decrease in bulk carbonate $\delta^{13}C$ values, but *before* the benthic foraminiferal extinction at 54.989 Ma, as defined by Thomas (2003). Evenness values are significantly negatively correlated with kurtosis values within this higher-resolution window across the onset of the CIE ($R = -0.88$, $p < 0.01$).

Ostracode communities show a decrease in species richness (Fig. 2A), but the kurtosis pattern is subtly reversed relative to that of foraminifera. The highest kurtosis values occurred in the pre- and post-CIE periods, and the lowest kurtosis values occurred in the later part of the CIE interval (Fig. 2B, see caption for statistical significance). Ostracode community
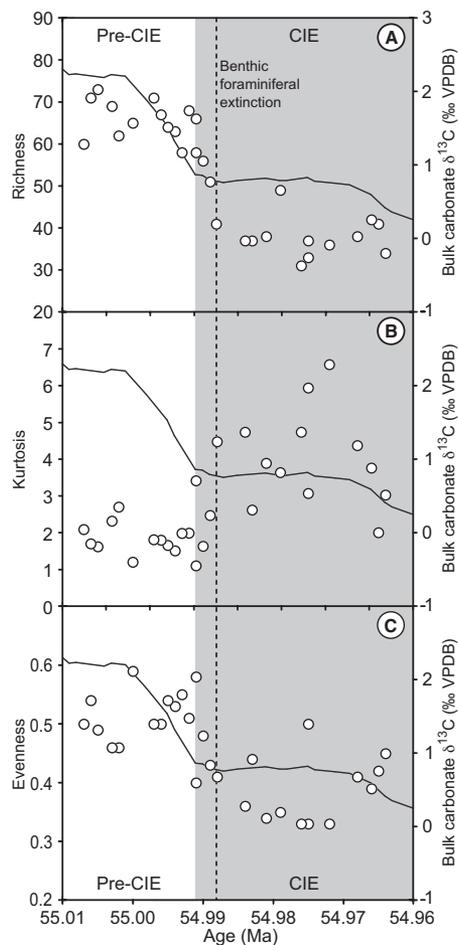
Figure 3. High-resolution benthic foraminiferal communities during the onset of the Paleocene-Eocene thermal maximum at Ocean Drilling Program Site 690. Shading is used to differentiate the different stages of the Paleocene-Eocene thermal maximum relative to the carbon isotope excursion (CIE) (from Thomas, 1990). Increasing kurtosis values indicate increasing stress before the recognized extinction (dashed vertical line). When the high-resolution values are binned for the intervals before and after the benthic foraminiferal extinction horizon, kurtosis values are significantly greater above the extinction horizon (Student's one-tailed t-test, $p < 0.01$). This also holds true when the values are binned before and after the onset of the CIE ($p < 0.01$).

RACs were the most flat and convex-down in the latest part of the CIE. In contrast to the foraminifera, ostracode kurtosis and bulk carbonate $\delta^{13}C$ values are significantly positively correlated ($R = 0.62$, $p < 0.05$), and there is a similar apparent ecological threshold for kurtosis values around bulk carbonate $\delta^{13}C$ values of 1‰ (Student's one-tailed t-test, $p < 0.05$). Evenness is significantly negatively correlated with kurtosis ($R = -0.79$, $p < 0.01$), although the average evenness was lower during the post-CIE than the pre-CIE period (Fig. 2C).

DISCUSSION

Benthic foraminiferal communities became increasingly stressed just before and during the Paleocene-Eocene thermal maximum, and community reorganization occurred just before the taxonomically defined extinction. The pattern of RACs through time suggests that the climate perturbation induced the start of community changes before major taxonomic turnover. Kurtosis values may reflect a direct response to the changing environmental conditions as recorded by bulk carbonate $\delta^{13}C$ values, although the response did not appear until carbonate $\delta^{13}C$ values dropped below 1‰, suggesting the existence of some ecological threshold. Such a threshold would explain why the community response appears to follow the onset of the CIE and precede the benthic foraminiferal extinction, though these patterns and interpretations must be tempered by the time-averaged nature of bulk carbonate $\delta^{13}C$ values and the discretizing effects of defining intervals and horizons. Although ecological responses clearly operated across finer temporal resolutions than the observed sample resolution, the documented changes in foraminiferal RACs are significant.

In contrast, ostracode communities became less stressed during the same time interval. This marked difference between the response of foraminifera and ostracodes to the Paleocene-Eocene thermal maximum could have several explanations: (1) the record of the onset of the CIE (i.e., 55.01–54.96 Ma; Fig. 3) contains only one ostracode sample compared to 29 foraminifer samples (see the Appendix for explanation); it is conceivable that a highly stressed response was not preserved; (2) ostracode faunal samples were generally smaller and of more variable size than foraminiferal faunal samples; (3) Paleocene-Eocene thermal maximum environmental changes were more favorable to ostracodes, whether through resources, specific environmental conditions, or biotic interactions.

Regarding the first explanation, the general RAC patterns are very different for ostracodes and foraminifera, so it is unlikely that a higher resolution would change the broad pattern. Regarding the second explanation, although kurtosis is independent of sample-size, the smaller ostracode sample sizes may be less representative of the true population distribution. To test this hypothesis, each ostracode and foraminiferal assemblage was resampled to an abundance of 50 specimens (i.e., size of the smallest ostracode samples) without replacement 10,000 times. The resulting mean resampled kurtosis values are significantly positively correlated with the observed kurtosis values within each group ($R > 0.96$, $p < 0.01$); thus, differences in sample sizes within and among foraminiferal and ostracode assemblage cannot explain the differences in kurtosis trends. The most likely

explanation for the different responses of the two groups is that ostracode communities were actually less stressed by the Paleocene-Eocene thermal maximum, and some taxa may have benefited, although possibly indirectly, from rapid warming. This group-level difference in RAC patterns highlights the importance of examining multiple groups through intervals of extinction or major environmental change because conditions that are stressful for some groups may not be for others.

Evenness is positively correlated with kurtosis in both groups, which is expected given that an implicit hypothesis for RAC data is that a more disturbed community will show lower evenness. However, subtle differences in the trends of kurtosis and evenness can provide additional insight about the ecological impact of environmental changes. For example, foraminiferal communities became more even prior to the onset of the CIE, while kurtosis values remained stable (Fig. 2). This increase in evenness is not intuitive, because without the kurtosis pattern, an interpretation might suggest that communities were recovering from some unknown perturbation. During the post-CIE period, ostracode evenness was lower than would be predicted by a simple recovery to pre-CIE values, indicating higher levels of disturbance after the CIE than either before or during the CIE. Kurtosis values are similar for pre- and post-CIE communities, suggesting ostracode communities responded to the environmental changes before "recovering," similar to the pattern seen in foraminiferal communities.

CONCLUSIONS

Severe rapid global warming during the Paleocene-Eocene thermal maximum produced variable changes in community structure, partly independent of taxonomic loss, among deep-ocean foraminifera and ostracodes. Foraminiferal communities were highly stressed at the onset of the Paleocene-Eocene thermal maximum, as indicated by extinction (Thomas, 1990, 2003, 2007) and the RAC patterns presented here. In contrast, ostracode communities appear to have been less stressed, or at least more even, through the Paleocene-Eocene thermal maximum. RACs also indicate a recovery, or at least return toward pre-event community structure, in both groups.

RACs provide insight into community responses to the Paleocene-Eocene thermal maximum, and they have the potential to provide similar insight for other time intervals, such as the ongoing modern mass extinction (Myers et al., 2000). The results of this study underscore the reality that extinction events are the result of complex interactions rather than a single, simple cause. Our method promotes the construction of models for evolution

and extinction patterns that include ecological processes. Comparisons of RACs across an extinction interval offer an independent method to examine taxonomic and ecological impact. RACs have the potential to be adapted to a variety of systems. For example, modern ecosystems may be adversely affected without an immediate or obvious loss of taxa, and RACs have the potential to detect "early warning" signals through monitoring of current ecosystems and the ecological responses to global warming and other anthropogenic changes. The implication of this study for future climate change is that while taxonomic loss and community restructuring are likely to be unavoidable, some groups will thrive. This study presents a method to track these changes and detect the eventual recovery.

REFERENCES CITED

Bains, S., Corfield, R.M., and Norris, R.D., 1999, Mechanisms of climate warming at the end of the Paleocene: Science, v. 285, p. 724–727, doi: 10.1126/science.285.5428.724.

Bambach, R., Knoll, A., and Wang, S., 2004, Origination, extinction, and mass depletions of marine diversity: Paleobiology, v. 30, p. 522–542, doi: 10.1666/0094-8373(2004)030<0522:OEAMDO>2.0.CO;2.

Bazzaz, F.A., 1975, Plant species diversity in old-field successional ecosystems in southern Illinois: Ecology, v. 56, p. 485–488, doi: 10.2307/1934981.

Belaoussoff, S., and Kevan, P.G., 1998, Toward an ecological approach for the assessment of ecosystem health: Ecosystem Health, v. 4, p. 4–8, doi: 10.1046/j.1526-0992.1998.00066.x.

Bowen, G.J., Bralower, T.J., Delaney, M.L., Dickens, G.R., Kelly, D.C., Koch, P.L., Kump, L.R., Meng, J., Sloan, L.C., Thomas, E., Wing, S.L., and Zachos, J.C., 2006, Eocene hyperthermal event offers insight into greenhouse warming: Eos (Transactions, American Geophysical Union), v. 87, p. 165–169, doi: 10.1029/2006EO170002.

Dickens, G.R., 2003, Rethinking the global carbon cycle with a large, dynamic and globally mediated gas hydrate capacitor: Earth and Planetary Science Letters, v. 213, p. 169–183, doi: 10.1016/S0012-821X(03)00325-X.

Farley, K.A., and Eltgroth, S.F., 2003, An alternative age model for the Paleocene-Eocene thermal maximum using extraterrestrial ^{3}He: Earth and Planetary Science Letters, v. 208, p. 135–148, doi: 10.1016/S0012-821X(03)00017-7.

Gray, J.S., 1981, Detecting pollution-induced changes in communities using the log-normal distribution of individuals among species: Marine Pollution Bulletin, v. 12, no. 5, p. 173–176, doi: 10.1016/0025-326X(81)90230-7.

Halloy, S., and Barratt, B., 2007, Patterns of abundance and morphology as indicators of ecosystem status; a meta-analysis: Ecological Complexity, v. 4, p. 128–147, doi: 10.1016/j.ecocom.2007.04.002.

Hayek, L.C., and Buzas, M.A., 1997, Surveying Natural Populations: New York, Columbia University Press, 563 p.

Kelly, D.C., Zachos, J.C., Bralower, T.J., and Schellenberg, S.A., 2005, Enhanced terrestrial weathering/runoff and surface ocean carbonate production during the recovery stages of the Paleocene-Eocene thermal maximum: Paleoceanography, v. 20, p. 11, doi: 10.1029/2005PA001163.

Kennett, J.P., and Stott, L.D., 1991, Abrupt deep sea warming, palaeoceanographic changes and benthic extinctions at the end of the Paleocene: Nature, v. 353, p. 225–229, doi: 10.1038/353225a0.

McGhee, G.R., Jr., Sheehan, P.M., Bottjer, D.L., and Droser, M.L., 2004, Ecological ranking of Phanerozoic biodiversity crises: Ecologic and taxonomic severities are decoupled: Palaeogeography, Palaeoclimatology, Palaeoecology, v. 211, p. 289–297, doi: 10.1016/j.palaeo.2004.05.010.

McGill, B.J., Etienne, R.S., Gray, J.S., Alonso, D., Anderson, M.J., Benecha, H.K., Dornelas, M., Enquist, B.J., Green, J.L., He, F., Hurlbert, A.H., Magurran, A.E., Marquet, P.A., Maurer, B.A., Ostling, A., Soykan, C.U., Ugland, K.I., and White, E.P., 2007, Species abundance distributions: Moving beyond single prediction theories to integration within an ecological framework: Ecology Letters, v. 10, p. 995–1015, doi: 10.1111/j.1461-0248.2007.01094.x.

Myers, N., Mittermeier, R.A., Mittermeier, C.G., da Fonseca, G.A.B., and Kent, J., 2000, Biodiversity hotspots for conservation priorities: Nature, v. 403, p. 853–858, doi: 10.1038/35002501.

Roehl, U., Westerhold, T., Bralower, T.J., and Zachos, J.C., 2007, On the duration of the Paleocene-Eocene thermal maximum: Geochemistry, Geophysics, Geosystems, v. 8, p. Q12002, doi: 10.1029/2007GC001784.

Sepkoski, J., Bambach, R., Raup, D., and Valentine, J., 1981, Phanerozoic marine diversity and the fossil record: Nature, v. 293, p. 435–437, doi: 10.1038/293435a0.

Sluijs, A., Bowen, G.J., Brinkhuis, H., Lourens, L.J., and Thomas, E., 2007, The Palaeocene-Eocene thermal maximum super greenhouse: Biotic and geochemical signatures, age models and mechanisms of climate change, in Williams, M., Haywood, A.M., Gregory, F.J., and Schmidt, D.N., eds., Deep Time Perspectives on Climate Change: Marrying the Signal from Computer Models and Biological Proxies: London, Micropalaeontological Society–Geological Society, p. 323–351.

Svensen, H., Planke, S., Malthe-Sorenssen, A., Jamtveit, B., Myklebust, R., Eidem, T.R., and Rey, S.S., 2004, Release of methane from a volcanic basin as a mechanism for initial Eocene global warming: Nature, v. 429, p. 542–545, doi: 10.1038/nature02566.

Thomas, C.D., Cameron, A., Green, R.E., Bakkenes, M., Beaumont, L.J., Collingham, Y.C., Erasmus, B.F.N., de Siqueira, M.F., Grainger, A., Hannah, L., Hughes, L., Huntley, B., van Jaarsveld, A.S., Midgley, G.F., Miles, L., Ortega-Huerta, M.A., Peterson, A.T., Phillips, O.L., and Williams, S.E., 2004, Extinction from climate change: Nature, v. 427, p. 145–148, doi: 10.1038/nature02121.

Thomas, D.J., Zachos, J.C., Bralower, T.J., Thomas, E., and Bohaty, S., 2002, Warming the fuel for the fire: Evidence for the thermal dissociation of methane hydrate during the Paleocene-Eocene thermal maximum: Geology, v. 30, p. 1067–1070, doi: 10.1130/0091-7613(2002)030<1067:WTFFTF>2.0.CO;2.

Thomas, E., and 25 others, 1990, Late Cretaceous through Neogene deep-sea benthic foraminifers (Maud Rise, Weddell Sea, Antarctica), in Barker, P.E., et al., eds., Proceedings of the Ocean Drilling Program, Scientific Results, Volume 113: College Station, Texas, Ocean Drilling Program, p. 571–594.

Thomas, E., 2003, Extinction and food at the sea floor: A high-resolution benthic foraminifera record across the initial Eocene thermal maximum, Southern Ocean Site 690, in Wing, S.L., Gingerich, P.D., Schmitz, B., and Thomas, E., eds., Causes and Consequences of Globally Warm Climates in the Early Paleogene: Geological Society of America Special Paper 369, p. 319–332.

Thomas, E., 2007, Cenozoic mass extinctions in the deep sea; what disturbs the largest habitat on Earth?, in Monechi, S., Coccioni, R., and Rampino, M., eds., Large Ecosystem Perturbations: Causes and Consequences: Geological Society of America Special Paper 424, p. 1–24.

Trenberth, K.E., Jones, P.D., Ambenje, P., Bojariu, R., Easterling, D., Klein Tank, A., Parker, D., Rahimzadeh, F., Renwick, J.A., Rusticucci, M., Soden, B., and Zhai, P., 2007, Observations: Surface and atmospheric climate change, in Solomon, S., et al., eds., Climate Change 2007: The Physical Science Basis: New York, Cambridge University Press, p. 235–336.

Twitchett, R.J., 2006, The palaeoclimatology, palaeoecology and palaeoenvironmental analysis of mass extinction events: Palaeogeography, Palaeoclimatology, Palaeoecology, v. 232, p. 190–213, doi: 10.1016/j.palaeo.2005.05.019.

Whittaker, R.H., 1965, Dominance and diversity in land plant communities: Science, v. 147, p. 250–260, doi: 10.1126/science.147.3655.250.

Zachos, J.C., Wara, M.W., Bohaty, S., Delaney, M.L., Petrizzo, M.R., Brill, A., Bralower, T.J., and Premoli-Silva, I., 2003, A transient rise in tropical sea surface temperature during the Paleocene-Eocene thermal maximum: Science, v. 302, p. 1551–1554, doi: 10.1126/science.1090110.

Zachos, J.C., Rohl, U., Schellenberg, S., Sluijs, A., Hodell, D.A., Kelly, D.C., Thomas, E., Nicolo, M., Raffi, I., Lourens, L.J., McCarren, H., and Kroon, D., 2005, Rapid acidification of the ocean during the Paleocene-Eocene thermal maximum: Science, v. 308, p. 1611–1615, doi: 10.1126/science.1109004.

Zachos, J.C., Schouten, S., Bohaty, S., Quattlebaum, T., Sluijs, A., Brinkhuis, H., Gibbs, S.J., and Bralower, T.J., 2006, Extreme warming of mid-latitude coastal ocean during the Paleocene-Eocene thermal maximum: Inferences from TEX$_{86}$ and isotope data: Geology, v. 34, p. 737–740, doi: 10.1130/G22522.1.